ACS ENGINEERING Au
AN OPEN ACCESS JOURNAL OF THE AMERICAN CHEMICAL SOCIETY

pubs.acs.org/engineeringau
Article

Particle-Resolved CFD Simulation of Diluted Catalytic Fixed Bed Reactors for Formaldehyde Production

Martin Kutscherauer* and Gregor D. Wehinger*

Cite This: ACS Eng. Au 2025, 5, 284−297
Read Online

ACCESS | Metrics & More | Article Recommendations | Supporting Information

ABSTRACT: In catalytic fixed bed reactors for highly exothermic reactions, the bed is often diluted with inert particles to prevent thermal runaway and to distribute the reaction more homogeneously along the reactor length. The partial oxidation of methanol to formaldehyde is an example with high industrial relevance, in which diluted fixed beds are applied. In this work, particle-resolved computational fluid dynamics (PRCFD) simulations are conducted for the hotspot region (0−0.5 m) of an industrial scale fixed bed for formaldehyde production to systematically investigate the impact of dilution on integral reactor performance and locally distributed quantities, such as the temperature and catalyst effectiveness factor. PRCFD is the most detailed modeling approach for the simulation of diluted fixed beds since the spatial resolution of the fixed bed geometry allows the inert particles to be considered directly without the implementation of averaged activity factors. Different catalyst distributions have a significant effect on integral conversion, hotspot formation, and catalyst overheating while increasing the inert thermal conductivity has only a minor impact on heat transport and hence reaction. The difference between the maximum catalyst temperature of two different catalyst arrangements can reach 34 K. Finally, the present study demonstrates that even highly diluted fixed beds with industrial particle and tube dimensions are not suited to perform intrinsic kinetic measurements for the partial oxidation of methanol because of catalyst overheating (ΔT = 23.12 K) and pore diffusion limitation ($\eta_{i,\mathrm{FA}} < 0.5$).

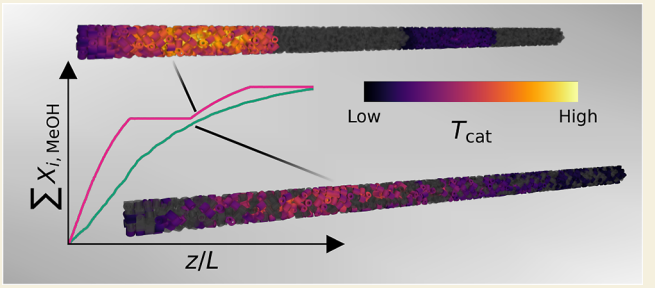

KEYWORDS: *reactor modeling, particle-resolved computational fluid dynamics, diluted catalytic fixed beds, transport phenomena, partial oxidation of methanol to formaldehyde*

1. INTRODUCTION

Heterogeneously catalyzed gas phase reactions are commonly performed in fixed-bed reactors.[1] For strong exothermal reactions over highly active catalysts, the fixed bed is often diluted with inert particles. Such reactions are commonly carried out in wall-cooled multitubular fixed-bed reactors. The major challenge in these reactors is heat management because it affects reactor performance and stability as well as catalyst lifetime. To efficiently remove the reaction heat while maintaining a low-pressure drop, slender tubes with a few particles over the tube diameter are used (tube-to-particle diameter-ratio $D/d_p < 6$). The dilution of the catalytic fixed bed with inert particles reduces the catalytic activity and consequently heat generation. Moreover, grading the dilution in the axial direction enables an overall more evenly distributed reaction and heat generation along the reactor.[2]

Formaldehyde is an important intermediate in the petrochemical industry and is used in the production of many resins, polymers, and adhesives. The partial oxidation of methanol to formaldehyde over an iron molybdate (Fe-Mo)catalyst is an example of an industrial process performed in a diluted catalytic fixed bed. This method, known as the FORMOX process, is the most important route to industrially produce formaldehyde, along with partial oxidation coupled with dehydrogenation of methanol over a silver catalyst.[3]

The FORMOX process is carried out in multitubular reactors cooled by high-temperature oil at 500−650 K. An excess of synthetic air containing 8−12 mol % oxygen is required for the feed, enabling inlet methanol concentrations of 6−10 mol %.[4] Due to the restriction of process safety, which only allows the operation of highly exothermic reactions below the explosion limit, the specific productivity of the process is low and offers significant potential for process intensification.[5−7] One common technique to optimize the productivity of a formaldehyde reactor is to introduce activity profiles by diluting the fixed bed due to its straightforward technical application.[8] Consequently, there is significant interest in gaining a deeper understanding of

Received: January 30, 2025
Revised: March 14, 2025
Accepted: March 19, 2025
Published: April 1, 2025

how dilution affects heat management and performance of an industrial-scale catalytic fixed bed for formaldehyde production.

Taniewski et al. experimentally tested diluted fixed beds (0−93.75 vol % inert particles) for oxidative coupling of methane in laboratory-scale reactors and found that the catalyst is more efficiently used.[9] Moreover, the hotspot of the reactor shifts toward the reactor outlet, becoming both lower and wider. Berger et al. conducted an experimental study to quantify the impact of catalyst distribution on conversion and on kinetic parameters estimated from the measurements for the catalytic decomposition of NO_2.[10−12] The prepared arrangements of inert and catalyst particles (0.0−80.0 vol % inert particles) in laboratory scale fixed bed reactors with large tube-to-particle diameter-ratio ($9 < D_t/d_p < 35$), ranges from vertically and horizontally segregated to perfectly mixed fixed beds.[10] The authors reported that various catalyst distributions affect the estimated kinetic parameters, especially for high conversion ($X_{NO_2} > 0.4$) and high dilution. Based on these studies, a criterion is derived to estimate the level of dilution and conversion at which the effect of dilution on the estimation of kinetic parameters is negligible.[10]

In addition to the experimental investigations, several authors presented numerical studies based on reaction engineering models. Based on the assumption of rotational symmetry, these models describe the tubular catalytic fixed bed as a pseudo-continuum discretized in axial (1D) or axial and radial directions (2D), upon which the governing equations are solved.[13] To model heat and mass transport, effective transport parameters calculated from semiempirical correlations are employed. In pseudo-continuum models, dilution can be implemented by scaling the reaction rates with an activity factor that describes the percentage of catalyst in a defined control volume.[14] Using layers with optimized lengths and catalyst activity factors can reduce the temperature of the hotspot, leading to improved reactor performance.[14−17] Moreover, the application of different diluted layers increases the thermal stability during dynamic operation and results in a lower parametric sensitivity of the system.[18−20] However, the advantages reported above of a diluted fixed bed are valid only under the assumption of a uniform activity profile with defined activity factors. In reality, the activity profile fluctuates and cannot be uniform due to the stochastic nature of a fixed bed.[21]

For the first time, Van Den Bleek et al. investigated the impact of fluctuation of activity by employing randomly distributed values of the activity factor and suggested a criterion to determine the influence of dilution on conversion as a function of the target activity level.[22] Sofekun et al. extended the criterion to more general cases.[23] Based on the statistical variation of the activity factor applied in a transient 1D pseudo-continuum model, Calverley et al. proposed that dilution of a fixed bed can result in thermal runaway, especially for highly diluted fixed beds with small D_t/d_p ratios.[24,25] Ganzer et al. utilized 3D packed bed geometries containing spherical inert and catalyst particles, synthetically generated through a Monte Carlo-based loading procedure, to extract realistic activity fluctuations in axial and radial directions.[21] The activity profiles are applied in a 1D and 2D pseudo-continuum model and the results are compared with an ideal uniform activity distribution.[26] The largest deviations from the ideal case were found in the hotspot temperature, and the authors derived a correlation to describe this deviation, which is mainly a function of the Stanton number (ratio between heat removal through the reactor wall and convective heat transport) and the third kind Damköhler number (ratio between heat production and convective heat transport).[26] Since the correlation is based on data calculated with pseudo-continuum models, which always make simplifying assumptions about the fixed bed geometry and the fluid flow, the authors did not recommend using the correlation as a design criterion and suggested employing more detailed modeling approaches such as particle-resolved computational fluid dynamic simulations (PRCFD).[26]

In contrast to pseudo-continuum models, in PRCFD simulations of diluted catalytic fixed beds, it is not necessary to model the dilution with an activity factor, since the spatial domain is fully resolved and every inert or catalyst particle is taken into account when solving the governing equations for momentum, mass, energy, and species mass.[27] Furthermore, the ability of PRCFD to consider the local structure and to accurately model the geometry of the packed bed is essential for the description of fixed beds with $D_t/d_p < 10$, in which the morphology of the packed bed is inhomogeneous and the simplifying assumptions of a pseudo-continuum model may result in inaccurate predictions.[28] Consequently, the PRCFD approach is a suitable method for a detailed numerical investigation of diluted catalytic fixed beds for highly exothermic reactions such as the partial oxidation of methanol to formaldehyde.

So far, only Shi et al. used PRCFD simulation to study how various catalyst arrangements affect temperature and conversion in a diluted fixed bed of cylinders however for the catalytic CO methanation.[29] The authors found that a catalyst distribution in which the degree of dilution decreases downstream can significantly reduce the hotspot temperature compared to a uniform distribution of catalyst particles, while integral performance remains almost unchanged. However, the packed bed investigated is only short (60 particles, $L/d_p = 8$) and cannot reflect the behavior of an industrial-scale fixed bed reactor. The impact of different catalyst configurations on spatially distributed quantities, such as temperature or catalyst effectiveness factors at the particle level and their relation to the integral reactor performance within an industrial scale diluted fixed bed, are still unknown. Although, this information is needed to determine the optimum dilution of a fixed bed for formaldehyde production.

In this work, the impact of catalyst distribution on integral performance data as well as local quantities is systematically studied for the hotspot region of an industrial scale diluted fixed bed for formaldehyde production (500 mm long fixed bed with 1186 ring-shaped particles, $D_t/d_{p,o} = 4.375$). On the basis of the simulation results, the correlation between the mixing index, which describes the homogeneity of the catalyst-inert mixture, and the integral methanol conversion and formaldehyde selectivity is investigated. The statistical fluctuations of local and integral quantities between different random catalyst distributions are also investigated. In addition to the different catalyst distributions, the effect of increasing the thermal conductivity of the inert particles in a diluted fixed bed on heat transport and consequently the catalytic reaction is analyzed. Diluted fixed beds are often used in kinetic studies to ensure isothermal operating conditions and to reduce other disturbing effects (e.g., dispersion and bypass).[12] Therefore, the suitability of a highly diluted fixed bed with industrial particle and reactor geometry for measuring formaldehyde kinetics is investigated by quantifying the relevant transport limitations.

https://doi.org/10.1021/acsengineeringau.5c00012
ACS Eng. Au 2025, 5, 284−297

2. METHODS

2.1. Geometry and Mesh Generation

The fixed bed containing 1186 hollow cylinders is generated synthetically with the rigid body approach implemented in the open-source game engine Blender 2.79.[30] A filling algorithm based on Partopour and Dixon is applied to fill the particles in a tube with a diameter of 21 mm.[31] The particles are injected separately with random positions and orientations in a space domain 50 mm above the tube. Due to gravity, the particles fall into the tube and fill it to the defined target height of 500 mm. Further details of the rigid body approach and the applied filling algorithm can be found in the literature.[32,33] The dimensions of the ring-shaped particles used ($d_{p,o} = h_p = 4.8$ mm, $d_{p,i} = 2.4$ mm) are typical for industrially scaled fixed bed reactors for formaldehyde production and result in a tube-to-particle diameter-ratio of $D_t/d_{p,o} = 4.375$. The synthetically generated fixed bed has a void fraction of 0.556. This value corresponds well to the void fraction of 0.575 measured in filling experiments carried out by Clariant AG with slightly larger steatite rings ($d_{p,o} = h_p = 5$ mm, $d_{p,i} = 2.6$ mm) in a tube of 22 mm diameter ($D_t/d_{p,o} = 4.4$).

In the next step, the bed geometry is discretized (meshing) for the subsequent Finite Volume Method within the PRCFD workflow.[34] The routine presented in Kutscherauer et al. is used to generate a polyhedral mesh in Siemens Simcenter STAR-CCM+ 2021.1.1.[34] Particle−particle and particle−wall contacts are locally modified to ensure high mesh quality while guaranteeing physical accuracy. The point and line contacts are replaced by a defined gap with a size of 0.8% of $d_{p,o}$ to enable the generation of mesh cells of the fluid phase in the contact region. Since diluted fixed beds contain two types of particles with different physical properties, the treatment of area contacts between particles needs to be modified. As already implemented in the original routine, particles of the same phase connected via an area contact are combined into one part of the domain.[34] In contrast, the contact surfaces of an area contact between two particles of different phases (inert and catalytically active) are merged to one surface (imprinting) so that a conformal mesh can be generated at the interface between the two particles of different domains. The differences in the mesh between combining and imprinting of area contacts are illustrated in Section S5 of the Supporting Information. The treatment applied to area contacts necessitates the generation of a new mesh for each different dilution, even if the geometry of the fixed bed remains unchanged. To enable the application of the conjugated mass and heat transfer model described in Section 2.2.3, a conformal mesh is generated not only at the catalyst−inert interface but also at the interfaces between fluid and catalyst, as well as between fluid and inert material. The base size, which is a characteristic parameter of the Siemens Simcenter STAR-CCM+ meshing algorithm, is set to 7 mm, and the mesh size at the particle surface is defined as 5% of the base size. At the outer surface of the particle and the wall of the tube, three layers of prismatic cells are introduced. As suggested by Dhole et al.,[35] the total thickness of the prism layers is set to the thickness of the momentum boundary layer δ_m in the stagnation point of a sphere, calculated according to Schlichting and Gersten[36]:

$$\frac{\delta_m}{d_p} = 1.13 Re_p^{-0.5} \tag{1}$$

with d_p is the diameter of a sphere with an identical specific surface and the particle Reynolds number Re_p:

$$Re_p = \frac{u_{in}\rho_f d_p}{\mu_f} \tag{2}$$

Moreover, three prism layers with a total thickness of 2 mm are generated at the inner particle surface. The resulting mesh comprises approximately 16.4 million cells in the fluid domain and 15.8 million cells in the inert and catalyst domains. For a slightly different fixed bed containing rings ($d_{p,o} = h_p = 5.6$ mm, $d_{p,i} = 2.3$ mm), Kutscherauer et al. have already proven that the mesh settings used result in a solution independent of the mesh size and contact modification.[34]

2.2. Governing Equations and Solving

Transport and reaction in the diluted catalytic fixed bed for formaldehyde production are described by steady-state governing equations for the fluid, catalyst, and inert domains. The three domains are coupled via fluid−catalyst, fluid−inert, and catalyst−inert interfaces. In addition to reactants and products, nitrogen is considered as an inert species since the feed of industrial formaldehyde reactors is commonly diluted.

2.2.1. Fluid Domain. In the fluid domain, the standard conservation equations are solved for the total mass, momentum, energy, and species mass. A detailed derivation of these equations can be found in many textbooks and publications.[37,38]

Conservation of the total mass:

$$\nabla\cdot(\rho_f \mathbf{u}) = 0 \tag{3}$$

Conservation of momentum:

$$\nabla\cdot(\rho_f \mathbf{u}\otimes\mathbf{u}) = -\nabla p + \nabla\cdot\mathbf{T} \tag{4}$$

with the viscous stress tensor $\mathbf{T}$:

$$\mathbf{T} = 2\mu_f\mathbf{D} - \frac{2}{3}\mu_f\nabla\cdot\mathbf{u}\mathbf{I} \tag{5}$$

with $\mathbf{D}$ being the deformation tensor:

$$\mathbf{D} = \frac{1}{2}[\nabla\mathbf{u} + (\nabla\mathbf{u})^T] \tag{6}$$

Conservation of energy:

$$\nabla\cdot(\rho_f \mathbf{u}h_{tot}) = \mathbf{u}\nabla p + (\mathbf{T}:\nabla\mathbf{u}) + \nabla\cdot(\lambda_f\nabla T) - \nabla\cdot\sum_{i=1}^{N}\rho_f D_{m,i}\nabla w_i h_i \tag{7}$$

with $h_{tot} = \sum_{i=1}^{N} w_i h_i$ as total mass specific enthalpy of the gas mixture and h_i as partial mass specific enthalpy of species i, which is defined as $dh_i = c_{p,i}dT$. Mechanical compression $\mathbf{u}\nabla p$, viscous dissipation $\mathbf{T}:\nabla\mathbf{u}$, and interdiffusion $\nabla\cdot\sum_{i=1}^{N}\rho_f D_{m,i}\nabla w_i h_i$ are considered, but their contribution to the energy conservation equation is small for all the cases studied.

Conservation of species mass:

$$\nabla\cdot(\rho_f \mathbf{u}w_i) = \nabla\cdot(\rho_f D_{m,i}\nabla w_i) \tag{8}$$

The species mass conservation is solved for $N-1$ species and the N^{th} species is computed via the definition that mass fractions sum to unity to guarantee total mass conservation. Since it is present in excess throughout the reactor, nitrogen is chosen as the N^{th} species.

The molecular diffusion coefficient $D_{m,i}$ of a component i in the gas mixture is calculated according to Fairbanks and Wilke[39] based on the binary diffusion coefficient determined using the semiempirical correlation of Fuller et al.[40] Furthermore, the mixture thermal conductivity λ_f, dynamic viscosity μ_f, and specific heat capacity $c_{p,f}$ are calculated by mass fraction weighting of the pure component data, while the molar weight of the mixture M_w is determined by molar fraction weighted averaging of the component molecular weights $M_{w,i}$. The density of the gas mixture is calculated via the ideal gas law:

$$\rho_f = \frac{pM_w}{\Re T} \tag{9}$$

In addition, the thermal conductivity, dynamic viscosity, and specific heat capacity of the pure components are computed as a function of the temperature using correlations suggested by the Design Institute of Physical Properties (DIPPR). Detailed information about the calculation of molecular diffusion coefficients and pure component properties is given in Section S1 of the Supporting Information.

2.2.2. Catalyst and Inert Domain. In this study, an Fe-Mo catalyst is employed for the synthesis of formaldehyde from methanol, as is commonly the case in industrial applications. Energy and species mass are transported only by diffusion within the porous catalyst particles. The catalyst domain is assumed as a pseudo-continuum and the transport is described via effective transport parameters.[41] Volumetric

https://doi.org/10.1021/acsengineeringau.5c00012
ACS Eng. Au 2025, 5, 284−297

energy and species mass source terms are used to implement the catalytic reaction.

Conservation of energy:

$$-\nabla\cdot(\lambda_{\text{eff}}\nabla T) = \rho_{\text{cat}} \sum_{j=1}^{N_{\text{react}}} \Delta H^{\circ}_{\text{react},j} r_j \tag{10}$$

with the specific molar standard reaction enthalpy $\Delta H^{\circ}_{\text{react},j}$, the molar reaction rate per catalyst mass r_j, the catalyst density ρ_{cat}, and the effective thermal conductivity λ_{eff} of the catalyst material.

Conservation of species mass:

$$-\nabla\cdot(\rho_{\text{cat,f}} D_{\text{eff},i}\nabla w_i) = \rho_{\text{cat}} M_{\text{w},i} \sum_{j=1}^{N_{\text{react}}} \nu_{i,j} r_j \tag{11}$$

with the density of the gas mixture inside the catalyst $\rho_{\text{cat,f}}$ and the stoichiometric coefficient $\nu_{i,j}$ of component i in reaction j. As outlined for the fluid domain, the species mass conservation equation is solved for $N - 1$ species and the N^{th} species (nitrogen) results from the definition that the mass fractions sum up to unity. The effective diffusion coefficient $D_{\text{eff},i}$ of species i is calculated based on the molecular diffusion coefficient $D_{\text{m},i}$ and the Knudsen diffusion coefficient $D_{\text{Kn},i}$ using the approximation of Bosanquet.[42] The equations used for the computation of $D_{\text{eff},i}$ and the required material properties of the catalyst are given in Section S2 of the Supporting Information.

The reaction network for the partial oxidation of methanol to formaldehyde, suggested by Deshmukh et al.[43] is shown in Figure 1.

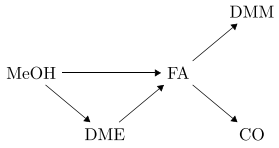

Figure 1. Reaction network of the partial oxidation of methanol to formaldehyde.[43]

Methanol (MeOH) can be directly oxidized to formaldehyde (FA), or it reacts via dimethyl ether (DME) as an intermediate. In consecutive reactions, FA could decompose and form carbon monoxide or react with methanol to dimethoxymethane (DMM). Water is formed as a byproduct in all of the reactions.

The molar reaction rates r_j for the five reactions are calculated with the kinetics model suggested by Deshmukh et al.[43] The rate equations were derived from measurements in a differentially operated reactor using a commercial Fe-Mo catalyst.[43] A detailed description of the applied kinetics model, the stoichiometry of the reactions, and their molar reaction enthalpies can be found in Section S3 of the Supporting Information.

The inert particles are impermeable for diffusive or convective species mass transport. Heat is transported only by thermal conduction, which reduces the energy conservation equation to:

$$-\nabla\cdot(\lambda_{\text{i}}\nabla T) = 0 \tag{12}$$

with the inert thermal conductivity λ_{i}. As described in Section 2.3, the value of λ_{i} is varied to study the influence of the inert thermal conductivity on the heat transport and reaction.

2.2.3. Coupling of Domains. Energy and species mass are diffusively transported across the interfaces of the different domains. Therefore, the conjugated heat and mass transfer model proposed by Kutscherauer et al. is applied to couple the domains.[41] Heat is transported across the fluid−catalyst, fluid−inert, and catalyst−inert interfaces, whereas species mass transfer occurs at the fluid−catalyst interface only. For further information on the model, the authors refer to Section S4 of the Supporting Information and the original publication by Kutscherauer et al.[41]

2.2.4. Boundary Conditions and Numerical Methodology. For the solution of the defined governing equations, an inlet temperature T_{in} and gas composition $y_{\text{in},i}$, as well as a uniformly distributed inlet velocity, are defined using a specified particle Reynolds number. Furthermore, a constant pressure of p_{out} is set at the outlet of the reactor tube. The tube wall is impermeable for the transport of species mass, and a no-slip boundary and a constant temperature T_{wall} are imposed as boundary conditions for fluid flow and heat transport, respectively. In addition, a no-slip boundary condition is defined at the outer particle surfaces to ensure that no heat or species mass is transported across the interfaces by convection. The catalyst-inert interface is set to be impermeable to species mass transport.

The simulations are carried out with the commercial software Siemens Simcenter STAR-CCM+ 2022.6. Details about the numerical methodology can be found in Kutscherauer et al.[41] Convergence is verified by monitoring residuals and the closure of the species mass and energy balance at all interfaces and throughout the reactor. All simulations are performed on 600 CPUs of the high-performance computing server bwUniCluster 2.0 with Intel Xenon Platinum 8358 processors at 2.6 GHz and 270 GB RAM. A simulation takes approximately five days to achieve convergence.

2.3. Simulation Setup and Design of the Parameter Study

The numerical study is divided into simulations to investigate the impact of catalyst distribution, inert thermal conductivity, and degree of dilution in a catalytic fixed bed for formaldehyde production. For all simulations performed, the fixed bed geometry and operating conditions remain unchanged to exclusively investigate the effect of dilution. The operating conditions listed in Table 1 are similar to those applied in the industry.[4] Consequently, the simulations reflect the first 500 mm of the catalytically active section in an industrial fixed bed, which corresponds to the hotspot region in which most of the methanol conversion occurs.

Table 1. Operating Conditions Used for the PRCFD Simulations (* Corresponds to DME, DMM, CO, FA, and H_2O)

parameter	value
$y_{\text{in,MeOH}}$	6.3×10^{-2}
$y_{\text{in,O}_2}$	8.9×10^{-2}
$y_{\text{in,N}_2}$	84.8×10^{-2}
$y_{\text{in},*}$	0.0
T_{in}	540 K
T_{wall}	540 K
Re_{p}	150
p_{out}	1 bar

Figure 2 shows the seven investigated catalyst distributions. The degree of dilution DoD, defined as the ratio between the amount of inert particles and the total number of particles, is kept constant at 0.5, for all the investigated catalyst arrangements. For the lateral case, the

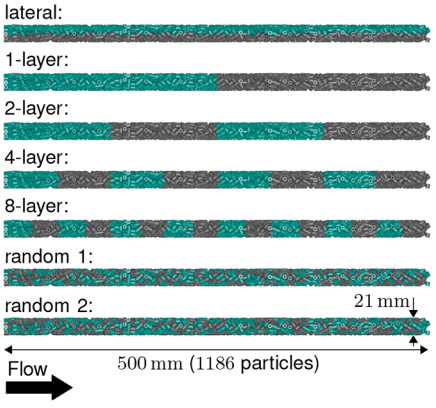

Figure 2. Investigated catalyst distributions.

https://doi.org/10.1021/acsengineeringau.5c00012
ACS Eng. Au 2025, 5, 284−297

particles are divided into an inert and a catalyst-containing volume divided by a plane through the center of the fixed bed. The four-layered arrangements are defined in such a way that every catalyst and inert layer has the same number of particles. If this is not possible, due to the predefined number of particles and the constant degree of dilution, the last catalytic and inert layer downstream contains a slightly reduced number of particles. The random catalyst distributions are generated by selecting which particles are catalytically active using the Mersenne-Twister pseudorandom number generator.[44]

To quantify the homogeneity of a catalyst distribution, the mixing index M is calculated according to Lacey[45]:

$$M = \frac{s_0^2 - s^2}{s_0^2 - s_r^2} \tag{13}$$

The variance s^2 of the catalyst distribution is calculated using the degree of dilution DoD_i of $N_s = 800$ samples with $n = 8$ particles selected from the entire fixed bed:

$$s^2 = \frac{1}{N_s - 1} \sum_{i=1}^{N_s} (\mathrm{DoD}_i - \mathrm{DoD}) \tag{14}$$

The samples are chosen by randomly selecting a particle and the $n - 1$ particles closest to it. A completely unmixed fixed bed has a variance of s_0^2 and s_r^2 is the variance of a completely random mixture:

$$s_0^2 = \mathrm{DoD}(1 - \mathrm{DoD}) \tag{15}$$

$$s_r^2 = \frac{\mathrm{DoD}(1 - \mathrm{DoD})}{n} \tag{16}$$

The effect of the degree of dilution is investigated by increasing DoD to 0.8 and 0.95. The catalyst particles in the higher diluted fixed beds are randomly distributed to allow comparison with the random 1 catalyst arrangement (DoD = 0.5). In all simulations of different catalyst distributions and dilution levels, the inert thermal conductivity is set to 2 W m^{-1} K^{-1}, which is the effective thermal conductivity λ_{eff} of the catalyst particles. To study the effect of inert thermal conductivity, this value is increased to 54 W m^{-1} K^{-1} (corresponding to carbon steel[46]) and 120 W m^{-1} K^{-1} (corresponding to brass[46]) for the random 1 catalyst arrangement.

3. RESULTS AND DISCUSSION

3.1. Impact of Catalyst Distribution

The overall coordination number CN is defined as the number of particles in contact with the investigated particle. Evaluating CN for each particle in the investigated fixed bed results in a mean coordination number of 3.96, with a standard deviation of 1.31. The coordination number is Gaussian distributed, as proven by a Shapiro−Wilk test.[47] The cumulative distribution of CN, the orientation distribution of the rings, and the axial and radial void fraction profile of the fixed bed are shown in Section S6 of the Supporting Information. The catalyst coordination number $\mathrm{CN_{cat}}$ is the number of catalyst particles that are in contact with the screened particle. The cumulative distribution of $\mathrm{CN_{cat}}$ considering all particles in the fixed bed is shown in Figure 3 for the investigated catalyst distributions. In this figure, a Gaussian distribution is assumed in the interval between $\mathrm{CN_{cat}}$ and $\mathrm{CN_{cat}} + 1$ to compare the discrete distribution of $\mathrm{CN_{cat}}$ with a continuous distribution. The mean values of $\mathrm{CN_{cat}}$ and their standard deviations are listed in Table 2. The catalyst coordination numbers of the two random catalyst arrangements are Gaussian distributed, which is confirmed by the Shapiro−Wilk test.[47] For the 1-layer case, approximately 50% of the particles are not in contact with a catalytic active particle. Adding more catalyst layers decreases the percentage of particles with $\mathrm{CN_{cat}} = 0$ and results in distributions and standard deviations of

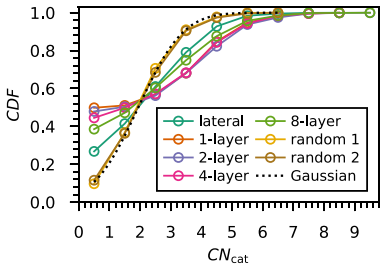

Figure 3. Cumulative density function of the catalyst coordination number for all investigated catalyst distributions.

$\mathrm{CN_{cat}}$ closer to the random catalyst arrangements. The $\mathrm{CN_{cat}}$ distribution and standard deviation of the lateral case are most similar to those of the random cases. The mean values of the catalyst coordination number are about half the overall CN and are not significantly affected by the catalyst arrangement.

A mixing index M calculated according to Lacey[45] close to one indicates that the random catalyst arrangements correspond to ideal homogeneous mixtures. The relatively low value of M of the 1-layer case demonstrates that the catalyst and inert particles are almost completely segregated, as expected. Although a growing number of layers leads to an increase in the mixing index, the mixing for the lateral case is still twice as high due to the larger interface between the catalytic and inert volumes.

The pressure drops for all studied catalyst distributions ranged from 41.19 to 41.59 mbar. The slight pressure drop deviations between the different cases are attributed to the differences in the gas phase composition, temperature, and consequently the gas density. Similar pressure drops and radial velocity profiles of the flow components shown in Section S7 of the Supporting Information indicate that the flow regimes remain practically unchanged between the various catalyst arrangements.

3.1.1. Impact on Temperature Distribution. Table 2 lists the maximum temperatures and catalyst temperature relative standard deviations that can be observed in a catalyst particle. Figure 4 shows the axial profiles of the circumferentially and radially averaged fluid temperatures and the mean temperatures of every particle. In addition, the temperatures at a plane section through the packed beds are given in Figure 5 to provide an illustrative representation of the local temperature fields. In the two different random catalyst distributions, the mean temperatures of the catalytic particles and $T_{cat,max}$ are similar, whereas the fluid temperature in the hotspot region $(0 < z/L < 0.4)$ differs up to 10 K between the two cases. Nevertheless, the standard deviation of the radially and circumferentially averaged fluid temperatures is as high as 15 K for both cases, as illustrated in detail in Section S7 of the Supporting Information. This indicates that the variation in the mean fluid temperatures between the random distributions is lower than the radial and circumferential temperature fluctuation in a cross-section area. The lateral catalyst arrangement results in a higher catalyst mean temperature and its maximum is located closer to the reactor inlet. However, the fluid mean temperature is similar to those of the random catalyst distributions, since the colder side with only inert particles is also considered in the averaging of the fluid temperature. The 1-layer and 2-layer cases have comparable catalyst and fluid temperatures in the hotspot region, which is approximately 30 K higher than the hotspot temperatures of the random distributions. Moreover, the hotspot regions of the random distributions are shifted downstream compared to the one- and two-layer cases. Due to the intermediate cooling in the

https://doi.org/10.1021/acsengineeringau.5c00012
ACS Eng. Au 2025, 5, 284−297

Table 2. Mean Catalyst Coordination Numbers, Their Standard Deviations, Mixing Indices, Maximum Catalyst Temperatures, Maximum Relative Standard Deviations of the Catalyst Temperature, Ratio between the Heat Dissipated through the Tube Wall and Heat Released by the Reaction, Methanol Conversions, and Formaldehyde Selectivities for All Investigated Catalyst Distributions

	lateral	1-layer	2-layer	4-layer	8-layer	random 1	random 2
CN_{cat} (mean)	2.010	1.967	2.044	2.036	1.975	1.941	1.961
CN_{cat} (std. D.)	1.660	2.171	2.222	2.141	1.965	1.157	1.209
M	0.514	0.017	0.036	0.123	0.256	1.000	0.998
$T_{cat,max}$/K	637.7	663.6	663.6	653.4	637.2	629.0	629.2
max. r. std. D. T_{cat} /%	1.721	2.073	2.072	2.080	1.651	1.610	1.566
$\dot{Q}_{removed}/\dot{Q}_{react}$	0.954	0.990	0.987	0.976	0.971	0.965	0.963
X_{MeOH}	0.800	0.871	0.847	0.836	0.837	0.833	0.834
S_{FA}	0.972	0.961	0.967	0.973	0.975	0.976	0.975

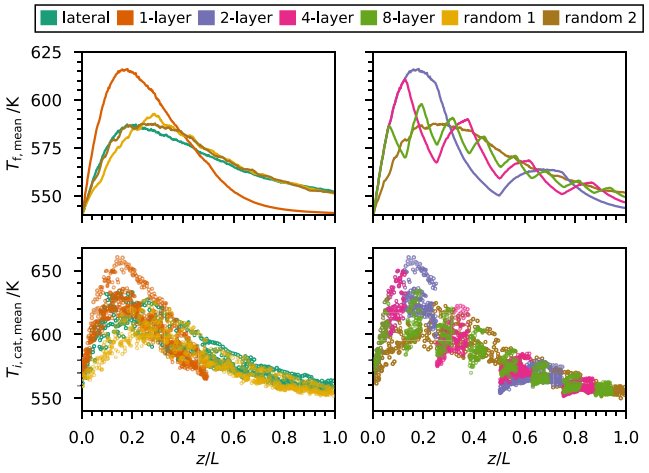

Figure 4. Axial temperature profiles of the circumferentially and radially averaged fluid temperatures (top) and the mean temperatures of each catalyst particle (bottom) for all investigated catalyst distributions.

inert sections, the introduction of four and eight catalyst layers results in a decrease in the average fluid and catalyst particle temperatures, and the profiles approach the random catalyst arrangements with a growing number of layers. Nevertheless, for all layered cases, steep temperature gradients in the axial direction can be observed at the beginning of each catalyst section close to the inlet where the methanol partial pressure is still high. This can be attributed to the high activity of the catalyst and the strong exothermicity of the reactions.

The ratio between the heat dissipated through the tube wall $\dot{Q}_{removed}$ and heat released by the reaction $\dot{Q}_{react}$, given in Table 2, provides a quantitative and integral assessment of the percentage of reaction heat removed from the cooling tube wall. Since steeper radial temperature gradients result in enhanced conductive heat transport toward the tube wall, the ratio $\dot{Q}_{removed}/\dot{Q}_{react}$ declines with an increasing number of layers and approaches the value of the random catalyst distributions. In the lateral catalyst arrangement, only half of the cooling tube wall is in close proximity to the heat-releasing catalyst particles, as illustrated in Figure 5. Consequently, the value of $\dot{Q}_{removed}/\dot{Q}_{react}$ is smaller than that for the layered and random catalyst distributions. Nevertheless, the $\dot{Q}_{removed}/\dot{Q}_{react}$ ratios of the different catalyst distributions differ only slightly, since for the investigated Reynolds number (Re_p = 150) the contribution of conduction to heat transport is small, as can be seen in Section 3.2.

For all investigated cases, the catalyst particles overheat in the hotspot region. The largest difference between the maximum mean temperature of the fluid and the maximum mean catalyst temperature can be observed for the lateral case (ΔT = 47.0 K) followed by the 1- and 2-layer arrangements (ΔT = 44.4 K). The particle overheating becomes smaller with a growing number of layers and reaches its minimum for the random distributions

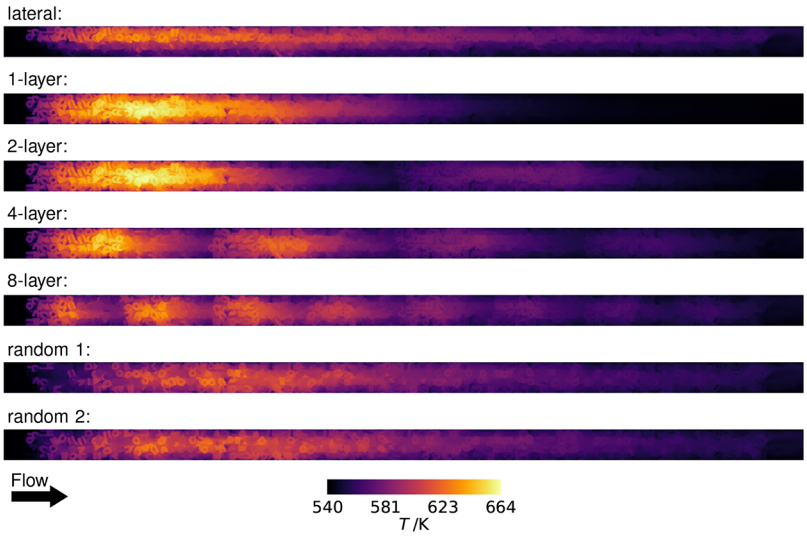

Figure 5. Temperatures on a plane through the fixed bed center for various catalyst distributions.

https://doi.org/10.1021/acsengineeringau.5c00012
ACS Eng. Au 2025, 5, 284−297

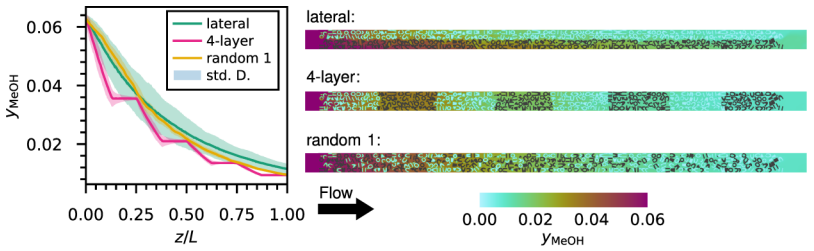

Figure 6. Axial profiles of the circumferentially and radially mass flux averaged methanol molar fractions with their standard deviations (left) and methanol molar fractions at a plane through the center of the fixed bed (right) for various catalyst distributions.

(33.9−37.2 K). Figure 5 shows that the particles with the highest overheating are located in the center of the packed bed, emphasizing that radial heat transport to the tube wall is limited. The maximum relative standard deviations of the mean particle temperatures are similar for all investigated catalyst distributions and range from 1.566% (random 2) to 2.080% (4-layer). The highest relative standard deviations are reached in the hotspot region, as shown in Section S7 of the Supporting Information. The difference between the maximum and minimum temperature within a particle is 52.0−52.4 K in the hotspot of the 1- and 2-layer arrangements and decreases with the growing number of layers toward 38.0−38.8 K for the random catalyst distributions. Such steep temperature gradients are mainly found in particles close to the cooling tube wall. The axial profile of the temperature range within each particle is given in Section S7 of the Supporting Information.

The investigation of the temperature distributions shows that particle overheating and the difference between the maximum and minimum temperatures are significantly lower for the random catalyst distributions. Moreover, it can be summarized that a higher mixing index leads to lower mean fluid and catalyst temperatures. Lowering the catalyst temperature can increase the catalyst lifetime, as it reduces the sintering and sublimation of molybdenum oxide.[48] However, the temperature increases by approximately 89 K from the inlet to the hottest point in a catalyst particle, even for random catalyst distributions.

To compare how this temperature increase changes in 1D and 2D pseudohomogeneous reactor models, the spatially resolved temperatures from the PRCFD simulations can be averaged over the three different domains circumferentially and radially (1D) as well as only circumferentially (2D). The resulting averaged temperatures and the corresponding standard deviation distributions are given in Section S7 of the Supporting Information for the case random 1. For the 1D profile, the maximum temperature is 29.7 K lower than in the spatially resolved temperatures. The highest standard deviations can be found in the hotspot region, reaching a value of 17.3 K. In contrast, the maximum temperature of the resolved distribution is only 5.8 K higher than the maximum of the circumferentially averaged 2D temperatures. However, the maximum standard deviation remains at 13.9 K in the hotspot region. This shows that the rotational symmetry approximation of a catalytic fixed bed used for a 2D pseudo-continuum is questionable for small tube-to-particle diameter ratios and highly exothermic and endothermic reactions, as already pointed out by Dixon.[28] This effect is further enhanced by the randomly distributed inert domain in the diluted fixed beds.

3.1.2. Impact on Integral Reactor Performance. The integral conversions of methanol and selectivities to formaldehyde are given in Table 2. The methanol conversion ranges from 0.800 to 0.871, while the formaldehyde selectivity is between 0.961 and 0.976. The observed high selectivity levels even at high conversions are typical for formaldehyde production from methanol over a Fe-Mo catalyst.[49,50] The fixed bed with only one catalytic layer results in the highest conversion and the lowest selectivity. Introducing additional catalytic layers results in a decline in conversion and improvement in selectivity due to the decrease in temperature, as described in Section 3.1.1. In accordance with the findings of Ganzer and Freund, the variation of integral conversion and selectivity between the random distributions is minimal.[26] Whereas the conversion of the lateral catalyst arrangement is significantly lower compared to all other investigated cases. Surprisingly, the selectivity of the lateral catalyst arrangement remains lower than that observed for the random and 8-layer catalyst distributions. This can be attributed to the partial bypassing of fluid flow around the catalyst in the axial direction. The bypassing is illustrated by the axial profile of the radially and circumferentially averaged methanol mole fractions and the methanol mole fraction on a plane through the fixed bed center, shown in Figure 6 for three catalyst arrangements and for all investigated cases in Section S7 of the Supporting Information. A certain part of the fluid cannot interact with the catalyst as it flows through the reactor, leading to higher concentrations of methanol at the inert side of the fixed bed and a decline in integral conversion. The cross-sectional variation of the methanol concentration is reflected in the higher standard deviation of the radially and circumferentially averaged methanol mole fraction compared with the other catalyst arrangements. Although convective and diffusive transport of methanol in radial and tangential directions reduces the maldistribution of methanol due to bypassing, it cannot completely compensate for it at the investigated Re_p of 150. The negative impact of bypassing in lateral catalyst distributions on conversion is in good agreement with the experimental results of Berger et al.[11]

Figure 7 shows the integral conversion and selectivity plotted versus the mixing indexes of the various catalyst distributions. For the layer catalyst arrangements, the conversion decreases and the selectivity increases with growing mixing index, and both approach asymptotically the value of a random mixed packed bed. At a mixing index of 0.256, corresponding to the 8-layer case, both conversion and selectivity differ only slightly from the random catalyst distribution (M = 1.000). The lateral catalyst distribution exhibits distinct behavior with a lower conversion and selectivity than that of the layer arrangements despite a higher mixing index. This indicates that the integral reactor performance of a catalyst distribution is not only a function of the mixing index. Accordingly, although the random arrangements result in the highest conversion and selectivity observed in this study, it is possible that more inhomogeneous distributions exist with better integral performance. Different

https://doi.org/10.1021/acsengineeringau.5c00012
ACS Eng. Au 2025, 5, 284−297

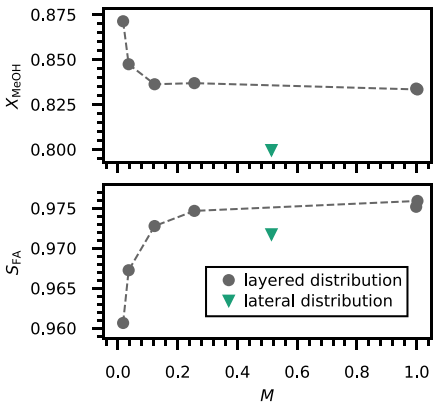

Figure 7. Methanol conversion (top) and formaldehyde selectivity (bottom) vs mixing index.

authors have already claimed to apply fixed beds with layers of varying degrees of dilution to achieve optimal reactor performance.[18,51,52]

3.1.3. Impact on Local Catalyst Performance. To investigate the local performance of the catalyst particles, the catalyst effectiveness factors $\eta_{i,FA}$ for the reaction of methanol to formaldehyde, the conversions of methanol $X_{i,MeOH}$ and the formaldehyde selectivities $S_{i,FA}$ are computed for each individual particle in the different fixed beds. The catalyst effectiveness factor of the individual pellet is calculated based on the volume-averaged reaction rate over the particle volume and the area-averaged reaction rate at the catalyst surface:

$$\eta_{i,FA} = \frac{\frac{1}{V_p}\int_V r_{MeOH,FA}\,dV}{\frac{1}{A_p}\int_A r_{MeOH,FA}\,dA} \tag{17}$$

The methanol conversion $X_{i,MeOH}$ and the formaldehyde selectivity $S_{i,FA}$ of each catalyst particle are determined using the volumetric species mass source terms $\dot{S}_i$ integrated over the particle volume:

$$X_{i,MeOH} = \frac{\int_V \dot{S}_{MeOH} M_{w,MeOH}^{-1}\,dV}{\dot{M}_{in,MeOH} M_{w,MeOH}^{-1}} \tag{18}$$

$$S_{i,FA} = \frac{\int_V \dot{S}_{FA} M_{w,FA}^{-1}\,dV}{\int_V \dot{S}_{MeOH} M_{w,MeOH}^{-1}\,dV} \tag{19}$$

Figure 8 shows the axial profiles of $\eta_{i,FA}$, $X_{i,MeOH}$, and $S_{i,FA}$ as well as the cumulative methanol conversions along the reactor for various catalyst distributions. The axial profiles of these quantities for all investigated cases are given in Section S7 of the Supporting Information.

The high reaction rate to formaldehyde due to the high activity of the catalyst, combined with the slow mass transport of species by pore diffusion within the particles, results in a low level of effectiveness factors along the reactor for all catalyst distributions studied. This demonstrates that the formaldehyde production rate of a catalyst particle is limited by pore diffusion, and most of the FA formation from methanol occurs close to the outer surface of the catalyst. These findings align well with the results reported by Partopour and Dixon.[53] The effectiveness factor calculated based on the Thiele modulus ϕ according to Aris[54] by assuming an isothermal pellet and a first-order reaction in methanol is 0.51 for the inlet conditions. In the PRCFD simulations, the effectiveness factors of the first particles in the fixed bed have a lower value (≈0.44), which is mainly due to catalyst overheating, as detailed in Section 3.1.1. In every situation, the effectiveness factor declines from the inlet to the hotspot and then begins to increase. Due to the decreasing partial pressure of methanol and oxygen, the reaction rate to

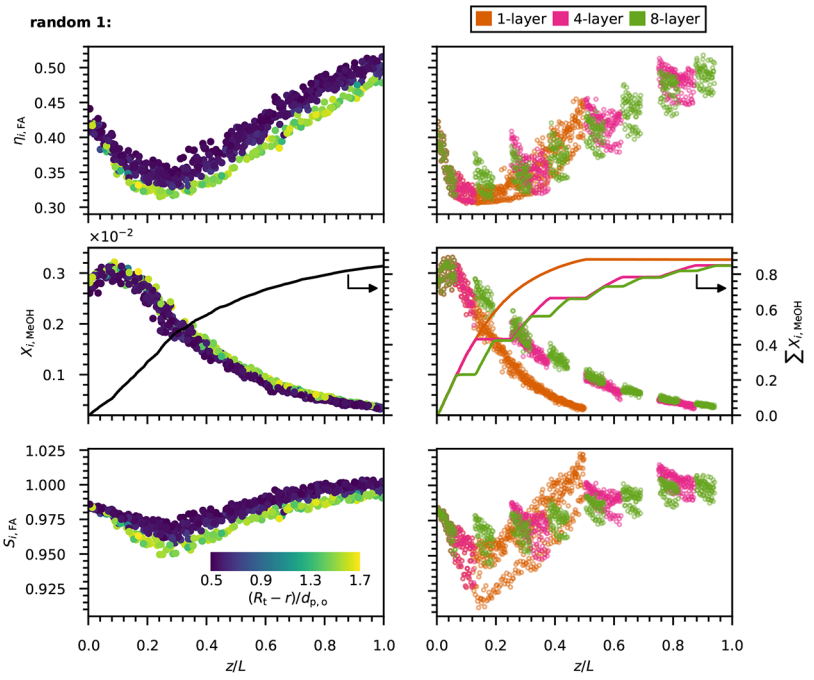

Figure 8. Axial profiles for various catalyst distributions of the particle-wise evaluated effectiveness factors of the methanol to formaldehyde reaction (top), the cumulative methanol conversions as well as the methanol conversions (middle), and the selectivities to formaldehyde (bottom) for all particles. The color of the dots for the random catalyst distribution (left) represents the radial position of the particle.

https://doi.org/10.1021/acsengineeringau.5c00012
ACS Eng. Au 2025, 5, 284−297

formaldehyde decreases, leading to a higher value of $\eta_{i,FA}$ at the outlet than at the inlet. Moreover, the lower temperature of particles close to the cooling tube wall results in a radial enhancement of the effectiveness factor toward the tube wall.

For the one-layer case, $\eta_{i,FA}$ is slightly lower than for random catalyst arrangements, and the minimum is shifted upstream similarly to the hotspot position, as described in Section 3.1.1. By increasing the number of catalyst layers, the profiles approach the values of a random catalyst arrangement. However, the effectiveness factor declines rapidly within one layer, which can be attributed to the steep temperature gradients in this region (see: Section 3.1.1).

For all investigated arrangements, the particle conversions increase from the inlet. The decrease in the fluid methanol concentration with contact time causes the maximum of $X_{i,MeOH}$ to be reached before the hotspot region. The catalyst particles in the center of the fixed bed have higher conversions compared to the particles near the tube wall because of the temperature variation in the radial direction. Nevertheless, the radial scattering is less pronounced than that of the effectiveness factor, which indicates that the particle-related conversion is only slightly affected by the steep radial temperature gradients. The highest radial differences in $X_{i,MeOH}$ can be observed for the lateral case due to the varying availability of methanol in the fluid phase caused by the bypassing effect described in Section 3.1.2. In the one-layer case the cumulative conversion gradient is the steepest since all catalyst particles are located in one cluster in this configuration. The layered arrangements become more similar to the $X_{i,MeOH}$ and cumulative conversion profiles of the random distributions with increasing numbers of layers.

In general, the particle-related formaldehyde selectivity decreases toward the hotspot region, reaches a minimum, and then increases downstream. In the rear half of the fixed bed, lower temperatures result in lower reaction rates for the reactions to CO and DMM, and additional formaldehyde is formed from DME in the downstream sections. Since the particle-wise formaldehyde selectivity is only related to formaldehyde conversion, the additional FA formed from DME can cause $S_{i,FA}$ to be slightly higher than one near the end of the catalytic fixed bed. This is especially the case for the distributions with one and two catalytic layers, in which higher amounts of DME are formed in the hotspot region, as shown in the axial DME mole fraction profile given in Section S7 of the Supporting Information. Because of the radially decreasing temperature, the selectivity of particles located in the center of the fixed bed is lower than that of particles in close proximity to the tube wall. This effect is more pronounced for the 1- and 2-layer cases, due to the steeper radial temperature gradients. The large scattering of the selectivity for these catalyst distributions leads to single catalyst particles in the fixed bed center, which have significantly lower selectivities than particles at the same axial position in the random catalyst arrangements. Unlike particle-wise conversion, the formaldehyde selectivity of a particle is strongly influenced by the local temperature to which it is exposed. As already observed for the axial profiles of $\eta_{i,FA}$, $X_{i,MeOH}$, and the cumulative conversion, the layered catalyst distributions approach the $S_{i,FA}$ profiles of the random catalyst arrangement by adding more catalytic layers.

3.2. Impact of Inert Particle Thermal Conductivity

Table 3 lists the maximum catalyst temperature, the maximum relative standard deviation of the temperature within one catalyst particle, the ratio between $\dot{Q}_{removed}$ and $\dot{Q}_{react}$, and the integral performance data of the catalyst arrangement random 1 with various inert thermal conductivities, i.e., 2, 54, and 120 W m^{-1} K^{-1}.

Table 3. Maximum Catalyst Temperatures, Maximum Relative Standard Deviations of the Catalyst Temperatures, Ratio between the Heat Dissipated through the Tube Wall and Heat Released by the Reaction, Methanol Conversions, and Formaldehyde Selectivities of the Catalyst Distribution Random 1 with Various Inert Particle Thermal Conductivities

λ_i/W m^{-1} K^{-1}	2	54	120
$T_{cat,max}$/K	629.0	625.0	624.4
max. r. std. D. T_{cat}/%	1.610	1.533	1.518
$\dot{Q}_{removed}/\dot{Q}_{react}$	0.965	0.966	0.967
X_{MeOH}	0.833	0.827	0.825
S_{FA}	0.976	0.977	0.978

A higher inert thermal conductivity results in an improved conductive heat transport to the tube wall, and the ratio between heat dissipated through the tube wall and heat released by the reaction increases. As a result, the temperatures of the fluid phase and catalyst particles decline with increasing inert thermal conductivity, as shown in Figure 9. Moreover, the maximum temperature relative standard deviation in one particle decreases. As a result of reduced temperatures, methanol conversion decreases with increasing inert thermal conductivity, while formaldehyde selectivity increases. However, the differences generated by the various inert thermal conductivities are small. An increase in inert thermal conductivity by a factor of 27 leads only to a reduction in the maximum catalyst temperature by 4 K. Other quantities, such as the particle-related effectiveness factor $\eta_{i,FA}$ or the axial molar fraction profile of methanol, are also only slightly affected by the inert thermal conductivity, as shown in Section S8 of the Supporting Information. The small effect of the inert thermal conductivity on heat transport and hence the reaction indicates that, for the Reynolds number studied (Re_p = 150), energy is predominantly transported by forced convection (lateral mixing) and the contribution of conductive heat transport plays only a minor role.[55,56]

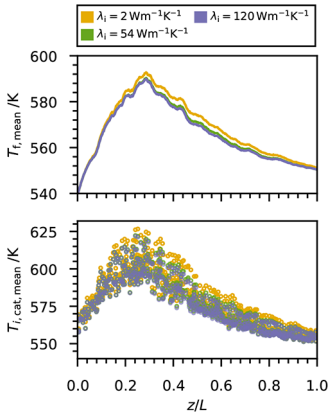

Figure 9. Axial temperature profiles of the circumferentially mass flux averaged fluid temperature (top) and the mean temperature of each catalyst particle (bottom) for catalyst distribution random 1 with various inert particle thermal conductivities.

https://doi.org/10.1021/acsengineeringau.5c00012
ACS Eng. Au 2025, 5, 284−297

3.3. Impact of Degree of Dilution

Three different degrees of dilution with a random catalyst distribution are investigated. The DoD = 0.5 corresponds to the case random 1. A mixing index of 1.000 shows that the mixture of catalyst and inert particles is also ideally homogeneous in the cases with DoD = 0.8 and 0.95. The maximum catalyst temperatures, the maximum relative standard deviations of the catalyst temperatures in a given particle, the ratio between $\dot{Q}_{removed}$ and $\dot{Q}_{react}$, and the performance data are listed in Table 4.

Table 4. Maximum Catalyst Temperatures, Maximum Relative Standard Deviations of the Catalyst Temperatures, Ratio between the Heat Dissipated through the Tube Wall and Heat Released by the Reaction, Methanol Conversions, and Formaldehyde Selectivities for Various Degrees of Dilution with Random Catalyst Distribution (DoD = 0.5 Corresponds to the Case Random 1)

DoD	0.5	0.8	0.95
$T_{cat,max}$/K	629.0	594.8	573.8
max. r. std. D. T_{cat}/%	1.610	0.811	0.463
$\dot{Q}_{removed}/\dot{Q}_{react}$	0.965	0.958	0.949
X_{MeOH}	0.833	0.511	0.155
S_{FA}	0.976	0.982	0.985

The increasingly smaller amount of catalyst results in a nonlinear decrease in methanol conversion and a linear increase in formaldehyde selectivity with increasing degree of dilution. In contrast to the notable reduction in conversion, the change in selectivity is only small, indicating that the applied Fe-Mo catalyst mainly promotes the formation of formaldehyde.[49,50] As shown in Figure 10, the mean temperatures of the fluid and

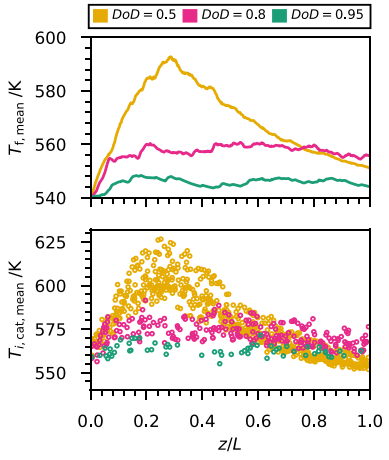

Figure 10. Axial temperature profiles of the circumferentially mass flux averaged fluid temperature (top) and the mean temperature of each catalyst particle (bottom) for various degrees of dilution with random distribution (DoD = 0.5 corresponds to the case of random 1).

catalyst decrease with increasing DoD. For DoD = 0.8 and 0.95, no distinct hotspots are formed. The average temperature of the fluid and catalyst rises abruptly at the inlet and stays almost constant throughout the reactor. Due to the smaller temperature gradients in the radial direction, the conductive heat transport toward the tube wall is reduced for higher degrees of dilution, and the ratio $\dot{Q}_{removed}/\dot{Q}_{react}$ decreases.

Although the fluid and catalyst temperatures increase only slightly, still the overheating of individual catalyst particles can be observed, as illustrated by the temperature on a plane through the fixed bed shown in Figure 11. However, the differences between the maximum mean temperature of the fluid and the catalyst decrease from 33.9 K (DoD = 0.5) to 30.83 K (DoD = 0.8) and 23.12 K (DoD = 0.95). Moreover, the relative standard deviations of the temperature of one catalyst particle and the temperature range within one particle are reduced with increasing degree of dilution, as given in Section S9 of the Supporting Information. In summary, a larger DoD decreases methanol conversion, and consequently, the amount of heat released and the temperature of the catalyst and fluid domain. Moreover, a higher degree of dilution results in smaller variations of temperature along the reactor length and between fluid and catalyst. However, even in highly diluted fixed beds (DoD = 0.95), the temperature in the catalyst particles can be approximately 30 K above the inlet temperature; therefore, it is not possible to assume an isothermal operation, which would be necessary for well-defined kinetic measurements.

Figure 12 shows the axial profiles of $\eta_{i,FA}$, $X_{i,MeOH}$, and $S_{i,FA}$ calculated according to eqs 17−19 and the cumulative conversions. The smaller amount of catalyst leads to a smaller increase in the cumulative conversion with a higher degree of dilution. As the dilution increases, the changes in temperature and the partial pressure of methanol along the axial direction diminish, and the reduction of $X_{i,MeOH}$ decreases. At DoD = 0.95, the particle-related conversion only slightly changes throughout the reactor, resulting in a linear increase in the cumulative conversion from the inlet to the outlet of the fixed bed. The small radial scattering of $X_{i,MeOH}$ is not affected by the variation in the degree of dilution. In contrast to the 0.5 dilution, the particle-related formaldehyde selectivity remains constant in the axial direction for DoD = 0.8 and 0.95. One reason for this is the smaller variation in temperature. Since there is no formation of hotspots for DoD = 0.8 and 0.95, no loss of selectivity can be observed after the inlet region. In addition, the missing hotspot leads to a reduced formation of DME, as shown in Section S9 of the Supporting Information. Therefore, unlike DoD = 0.5, the amount of DME converted to FA is reduced in the rear half of the reactor, and there is no increase in selectivity. As the radial temperature gradient becomes less pronounced, the radial scattering of $S_{i,FA}$ at the same axial position diminishes with an increasing degree of dilution. Moreover, the lower temperatures result in a slightly higher particle-related selectivity for DoD = 0.95, compared to DoD = 0.8. Analogous to $S_{i,FA}$, the axial distribution of $\eta_{i,FA}$ becomes more uniform for DoD = 0.8 and 0.95, different to DoD = 0.5, owing to the reduced temperature fluctuations along the reactor. However, the increase in the mean catalyst temperature at the inlet results in a small drop in the effectiveness factor at the beginning of the fixed bed for DoD = 0.8 and $\eta_{i,FA}$ is slightly lower compared to DoD = 0.95. At higher dilutions and reduced radial temperature gradients, the radial scattering of $\eta_{i,FA}$ becomes smaller, but the catalyst particles located in the vicinity of the tube wall still have higher catalyst effectiveness than the catalyst particles in the center of the fixed bed. For case DoD = 0.95, the effectiveness factor is determined based on the Thiele modulus, assuming an isothermal pellet and a first-order reaction.[54] In the calculation, the inlet gas composition and temperatures ranging from the minimum to the maximum catalyst mean temperature are used. The resulting range of effectiveness factors agrees well with the PRCFD results. This demonstrates that the approximation of

https://doi.org/10.1021/acsengineeringau.5c00012
ACS Eng. Au 2025, 5, 284−297

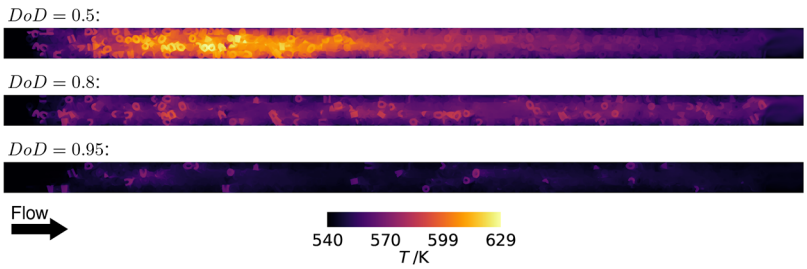

Figure 11. Temperatures at a plane through the fixed bed center for various degrees of dilution with random distribution (DoD = 0.5 corresponds to the case of random 1).

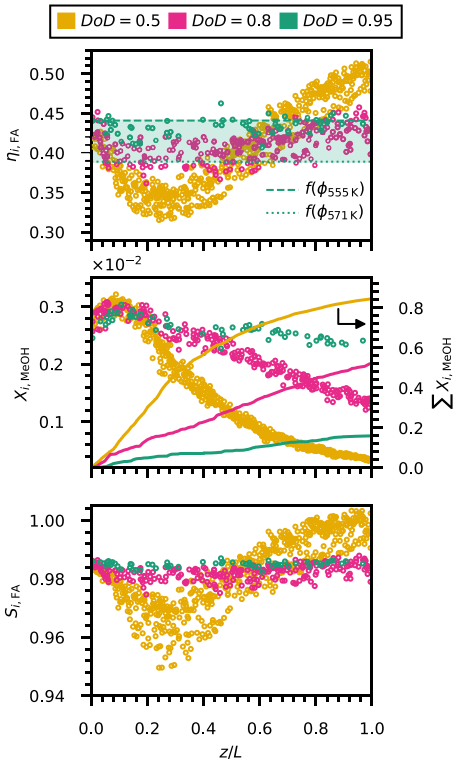

Figure 12. Axial profiles for various degrees of dilution (DoD = 0.5 corresponds to the case random 1) of the particle-wise evaluated effectiveness factor of the methanol to formaldehyde reaction (top), the cumulative methanol conversion as well as the methanol conversion (middle), and the selectivity toward formaldehyde (bottom) for each particle.

Aris[54] is able to predict the level of the effectiveness factor for a fixed bed of formaldehyde production, if dilution is high, conversion is low and the catalyst overheating is considered in the temperature applied for the calculation.

Diluted catalytic fixed beds are often used in kinetics measurement.[10−12] The investigations on the impact of the degree of dilution in a catalytic fixed bed for formaldehyde production show that catalyst overheating occurs even for a high dilution and the reactor cannot be assumed to be isothermal. Furthermore, transport limitation by pore diffusion can only be slightly reduced by a higher dilution, resulting in an effectiveness factor of about 0.45 for a DoD = 0.95. In conclusion, a diluted fixed bed with an industrial-scale tube and particle dimensions is not suitable for measuring the transport limitation-free kinetics of the partial oxidation of methanol to formaldehyde under the investigated operating conditions. However, the uniform and well-defined reaction conditions along the reactor allow the determination of effective kinetics for a catalyst particle based on experiments in a highly dilute fixed bed. For such kinetic measurements, it is essential to ensure that conversion remains low ($X_{\mathrm{MeOH}} \leq 0.155$) for all temperatures and gas compositions investigated by applying high degrees of dilution and sufficiently low residence times. Moreover, the temperature increase within the catalyst particles must be taken into account when determining the kinetic parameters from the experiments. It is important to note that when such effective catalyst particle kinetics is employed, the reaction and the limitation by pore diffusion are lumped together and the kinetic parameters are only valid for a specific catalyst particle shape and material.

4. CONCLUSIONS

In the presented work, the PRCFD approach coupled with heat transport within inert particles as well as heat and species mass transport and reaction within catalyst particles is used to simulate a diluted fixed bed for the production of formaldehyde from methanol. The influence of catalyst distribution, inert thermal conductivity, and degree of dilution on the temperature distribution as well as on integral and local performance quantities is examined, and the main findings are as follows:

1. The integral conversion and selectivity are affected by the overall and local catalyst arrangement. Random catalyst distributions correspond to an ideal homogeneous mixture and yield the best performance of the arrangements investigated in this study. However, conversion and selectivity are not only a function of mixing homogeneity. Catalyst distributions resulting in higher reactor performance are possible.
2. The hotspot temperature and the temperature range within one given particle strongly increase with increasing inhomogeneity of the catalyst particle distribution. The axial temperature profiles of the layered catalyst arrangements approach a random catalyst distribution with a growing number of layers.
3. The particle-related selectivity and effectiveness factors decline in the hotspot region. The lower hotspot temperature of the homogeneous random catalyst distribution leads to a smaller decrease in the particle-related selectivity and effectiveness factors in this region.
4. The thermal conductivity of inert particles has only a small influence on the temperature distribution, as well as on the integral and local reactor performance. This indicates that convective heat transport (lateral mixing) is more dominant than conductive heat transport under the industrial-relevant operation conditions investigated.
5. In all the cases studied, even for highly diluted fixed beds (DoD = 0.95), a pore diffusion limitation can be observed

https://doi.org/10.1021/acsengineeringau.5c00012
ACS Eng. Au 2025, 5, 284−297

resulting in a small catalyst effectiveness factor ($\eta_{i,FA}$ < 0.5).

6. Increasing the degree of dilution leads to a more uniform temperature distribution along the reactor without the formation of a hotspot and reduces the overheating of catalyst particles. However, the difference between the temperature within a catalyst particle and the inlet temperature can be about 30 K even at a high dilution of DoD = 0.95, so the reactor cannot be considered isothermal.
7. Due to catalyst overheating and pore diffusion limitation, diluted fixed beds with industrial scale tubes and particle dimensions are not suitable for performing intrinsic kinetic measurements for the partial oxidation of methanol to formaldehyde. However, an effective catalyst particle kinetics can be derived from experiments in a diluted fixed bed if a low methanol conversion is ensured by using a high degree of dilution and a sufficiently low residence time.

The results of this work are valid only for the studied particle geometry and D_t/d_p ratio. However, the investigated particle and reactor tube dimensions are typical for industrial applications with highly exothermic and endothermic reactions. For smaller D_t/d_p a higher influence of the catalyst distribution on reactor performance can be expected since the effects caused by the local packed bed structure are more pronounced.[24,25] In addition to different particle shapes and D_t/d_p ratios, future work must examine the effect of diluting the catalytic fixed bed with inert particles that differ in shape and size from the catalyst particles.

As reported in this study and the literature,[19,50,52] a homogeneous mixture of inert and catalyst particles may not result in optimal performance, and a method for computer-aided optimization of the catalyst distribution would be beneficial. Because such an optimization based on PRCFD simulations alone is not computationally feasible, a hybrid approach could be applied where optimal activity factor profiles are calculated with pseudo-continuum models and then used to predict the spatially resolved catalyst distribution for the PRCFD simulations. To further intensify heat transport, a better understanding of the underlying transport mechanisms is essential. Therefore, nonreactive PRCFD simulations must be performed to determine the percentage between conductive and convective heat transport.[57] Moreover, data from PRCFD simulations must be validated with spatially resolved experimental data and then used to improve pseudo-continuum models for diluted fixed beds by incorporating local effects such as flow bypass into the correlations of effective transport parameters, as these models are still used in everyday engineering practice due to their low computational cost.[58,59] In future studies, transient PRCFD simulation should be performed to verify the results of reaction engineering models in terms of thermal stability and parametric sensitivity of diluted fixed beds.[18−20]

■ ASSOCIATED CONTENT

Supporting Information

The Supporting Information is available free of charge at https://pubs.acs.org/doi/10.1021/acsengineeringau.5c00012.

Supporting Information with additional figures, tables, and details of the applied model.(PDF)

The Supporting Material with figure data, an STL file of the simulated fixed bed geometry, and the spatial distributions of the particle-wise catalyst effectiveness factor, methanol conversion, and formaldehyde selectivity as Blender file (https://doi.org/10.5281/zenodo.14758674)

■ AUTHOR INFORMATION

Corresponding Authors

Martin Kutscherauer − *Institute of Chemical Process Engineering, Karlsruhe Institute of Technology, 76131 Karlsruhe, Germany*; orcid.org/0000-0002-1892-2033; Email: martin.kutscherauer@kit.edu

Gregor D. Wehinger − *Institute of Chemical Process Engineering, Karlsruhe Institute of Technology, 76131 Karlsruhe, Germany*; Email: gregor.wehinger@kit.edu

Complete contact information is available at: https://pubs.acs.org/10.1021/acsengineeringau.5c00012

Notes

The authors declare no competing financial interest.

■ ACKNOWLEDGMENTS

The authors thank Oliver Richter, Maximilian Dochnahl, and Gerhard Mestl from Clariant AG for the fruitful discussions about the formaldehyde process. The authors acknowledge support by the state of Baden-Württemberg through bwHPC.

■ ABBREVIATIONS

DIPPR	Design Institute of Physical Properties
DME	dimethyl ether
DMM	dimethoxymethan
FA	formaldehyde
MeOH	methanol
PRCFD	particle-resolved computational fluid dynamic
r. std. D.	relative standard deviation
std. D.	standard deviation

Symbols

A_p	particle surface area [m^3]
CN	coordination number
c_p	specific heat capacity [J kg^{-1} K^{-1}]
D	deformation tensor [Pa]
D_i	diffusion coefficient of component i [m^2 s^{-1}]
$D_{Kn,i}$	Knudsen diffusion coefficient of component i [m^2 s^{-1}]
$D_{m,i}$	molecular diffusion coefficient of component i [m^2 s^{-1}]
DoD	degree of dilution
d_p	diameter of a sphere with identical specific surface [m]
$d_{p,i}$	hollow cylinder inner diameter [m]
$d_{p,o}$	hollow cylinder outer diameter [m]
$\Delta H^{\circ}_{react,\,j}$	specific standard enthalpy of reaction j [J $kmol^{-1}$]
h_i	partial enthalpy of component i [J kg^{-1}]
h_p	hollow cylinder height [m]
h_{tot}	total enthalpy [J kg^{-1}]
I	identity tensor [s^{-1}]
L	fixed bed length [m]
M	mixing index
M_w	molecular weight of the mixture [kg $kmol^{-1}$]
$M_{w,i}$	molecular weight of the component i [kg $kmol^{-1}$]
N	number of components
N_{react}	number of reactions
N_s	number of samples
n	sample size
p	pressure [Pa]

$\dot{Q}_{react}$	heat released by reaction [W]
$\dot{Q}_{removed}$	heat dissipated through the tube wall [W]
$\Re$	ideal gas constant: 8314 J K^{-1} $kmol^{-1}$
Re_p	particle Reynolds number: $Re_p = \frac{u_{in}\rho_f d_p}{\mu_f}$
r_j	rate of reaction j [kmol s^{-1} kg_{cat}^{-1}]
S_{FA}	integral formaldehyde selectivity
$S_{i,FA}$	formaldehyde selectivity of particle i
S_i	volumetric species mass source of component i [kg m^{-3} s^{-1}]
s^2	variance of the distribution
s_0^2	variance of an unmixed mixture
s_r^2	variance of a random mixture
$\mathbf{T}$	viscous stress tensor [Pa]
T	temperature [K]
$\mathbf{u}$	velocity vector [m s^{-1}]
V_p	particle volume [m^3]
w_i	mass fraction of component i
X_{MeOH}	integral methanol conversion
$X_{i,MeOH}$	methanol conversion of particle i
y_i	molar fraction of component i
z	axial position m

Greek Letters

δ_m	momentum boundary layer thickness [m]
$\eta_{i,FA}$	catalyst effectiveness factor of the reaction from methanol to formaldehyde for particle i
λ	thermal conductivity [W m^{-1} K^{-1}]
μ	dynamic viscosity [Pa s]
$\nu_{i,j}$	stoichiometric coefficient of component i in reaction j
ρ	density [kg m^{-1}]
ϕ	Thiele modulus

Subscripts

cat	catalyst
eff	effective
f	fluid
i	inert
in	inlet
out	outlet
wall	tube wall

REFERENCES

(1) Eigenberger, G.; Ruppel, W. *Ullmann's Encyclopedia of Industrial Chemistry*; John Wiley & Sons, Ltd, 2012.

(2) Ebner, J. R.; Keppel, R. A.; Mummey, M. J. High productivity process for the production of maleic anhydride. 1994, EP0593646A1.

(3) Reuss, G.; Disteldorf, W.; Gamer, A. O.; Hilt, A. *Ullmann's Encyclopedia of Industrial Chemistry*; John Wiley & Sons, Ltd, 2000.

(4) Brookes, C.; Wells, P. P.; Cibin, G.; Dimitratos, N.; Jones, W.; Morgan, D. J.; Bowker, M. Molybdenum Oxide on Fe2O3 Core−Shell Catalysts: Probing the Nature of the Structural Motifs Responsible for Methanol Oxidation Catalysis. *ACS Catal.* **2014**, *4*, 243−250.

(5) Massa, M.; Häggblad, R.; Hansen, S.; Andersson, A. Oxidation of methanol to formaldehyde on cation vacant Fe−V−Mo-oxide. *Appl. Catal. A Gen.* **2011**, *408*, 63−72.

(6) Ovchinnikova, E. V.; Chumachenko, V. A.; Valuiskikh, N. N. Influence of the process parameters on temperature conditions and productivity of multitubular reactor for methanol to formaldehyde oxidation. *Catal. Ind.* **2013**, *5*, 297−311.

(7) Patience, G. S.; Cenni, R. Formaldehyde process intensification through gas heat capacity. *Chem. Eng. Sci.* **2007**, *62*, 5609−5612.

(8) de Vekki, A. V.; Marakaev, S. T. Catalytic partial oxidation of methane to formaldehyde. *Russ. J. of Appl. Chem.* **2009**, *82*, 521−536.

(9) Taniewski, M.; Lachowicz, A.; Skutil, K.; Czechowicz, D. The effect of dilution of the catalyst bed on its heat-transfer characteristics in oxidative coupling of methane. *Chem. Eng. Sci.* **1996**, *51*, 4271−4278.

(10) Berger, R. J.; Pérez-Ramlérez, J.; Kapteijn, F.; Moulijn, J. A. Catalyst performance testing: the influence of catalyst bed dilution on the conversion observed. *Chem. Eng. J.* **2002**, *90*, 173−183.

(11) Berger, R. J.; Pérez-Ramlérez, J.; Kapteijn, F.; Moulijn, J. A. Catalyst performance testing: Radial and axial dispersion related to dilution in fixed-bed laboratory reactors. *Appl. Catal., A* **2002**, *227*, 321−333.

(12) Berger, R. J.; Pérez-Ramlérez, J.; Kapteijn, F.; Moulijn, J. A. Catalyst performance testing: bed dilution revisited. *Chem. Eng. Sci.* **2002**, *57*, 4921−4932.

(13) Froment, G. F.; Bischoff, K. B.; De Wilde, J. *Chemical reactor analysis and design*; Wiley, 1990.

(14) Nie, Y.; Witt, P. M.; Agarwal, A.; Biegler, L. T. Optimal Active Catalyst and Inert Distribution in Catalytic Packed Bed Reactors: ortho-Xylene Oxidation. *Ind. Eng. Chem. Res.* **2013**, *52*, 15311−15320.

(15) Sadhukhan, P.; Petersen, E. E. Oxidation of naphthalene in packed-bed reactor with catalyst activity profile: A design scheme for improved reactor stability and higher product yield. *AIChE J.* **1976**, *22*, 808−810.

(16) Pirkle, J., Jr.; Wachs, I. E. Activity profiling in catalytic reactors. *Chem. Eng. Progr.* **1987**, *83*, 29−34.

(17) Buchanan, J.; Sundaresan, S. Optimal catalyst distribution and dilution in nonisothernal packed bed reactors. *Chem. Eng. Commun.* **1987**, *52*, 33−51.

(18) Quina, M. M. J.; Quinta Ferreira, R. M. Model comparison and sensitivity analysis for a fixed bed reactor with two catalytic zones. *Chem. Eng. J.* **1999**, *75*, 149−159.

(19) Quina, M. M. J.; Quinta Ferreira, R. M. Thermal Runaway Conditions of a Partially Diluted Catalytic Reactor. *Ind. Eng. Chem. Res.* **1999**, *38*, 4615−4623.

(20) Luyben, W. L. Catalyst dilution to improve dynamic controllability of cooled tubular reactors. *Comput. Chem. Eng.* **2012**, *37*, 184−190.

(21) Ganzer, G.; Daniel, A.; Freund, H. Detailed geometrical analysis of statistical activity variations in diluted catalyst beds. *Chem. Eng. Res. Des.* **2019**, *148*, 102−118.

(22) Van Den Bleek, C. M.; Van Der Wiele, K.; Van Den Berg, P. J. The effect of dilution on the degree of conversion in fixed bed catalytic reactors. *Chem. Eng. Sci.* **1969**, *24*, 681−694.

(23) Sofekun, O. A.; Rollins, D. K.; Doraiswamy, L. K. A random particle model for catalyst dilution. *Chem. Eng. Sci.* **1994**, *49*, 2611−2620.

(24) Calverley, E. M.; Witt, P. M.; Sweeney, J. D. Reactor runaway due to statistically driven axial activity variations in graded catalyst beds. *Chem. Eng. Sci.* **2012**, *80*, 393−401.

(25) Calverley, E. M.; Witt, P. M.; Sweeney, J. D. Reactor runaway due to statistically driven axial activity variations in graded catalyst beds: Loading from pre-measured single tube aliquots. *Chem. Eng. Sci.* **2013**, *90*, 170−178.

(26) Ganzer, G.; Freund, H. Influence of statistical activity variations in diluted catalyst beds on the thermal reactor behavior: Derivation of an a priori criterion. *Chem. Eng. Sci.* **2020**, *220*, No. 115607.

(27) Dixon, A. G.; Partopour, B. Computational Fluid Dynamics for Fixed Bed Reactor Design. *Annu. Rev. Chem. Biomol. Eng.* **2020**, *11*, 109−130.

(28) Dixon, A. G. Local transport and reaction rates in a fixed bed reactor tube: Exothermic partial oxidation of ethylene. *Chem. Eng. Sci.* **2021**, *231*, No. 116305.

(29) Shi, Y.; Li, H.; Chen, H.; Zhao, Y.; Cao, Y.; Liu, X.; Duan, X.; Qian, G.; Zhou, X. Thermal management of natural gas production from coke oven gas by optimizing catalyst distribution and operation conditions. *Chemosphere* **2023**, *327*, No. 138536.

(30) Flaischlen, S.; Wehinger, G. D. Synthetic Packed-Bed Generation for CFD Simulations: Blender vs STAR-CCM+. *ChemEngineering* **2019**, *3*, 52.

https://doi.org/10.1021/acsengineeringau.5c00012
ACS Eng. Au 2025, 5, 284−297

(31) Partopour, B.; Dixon, A. G. An integrated workflow for resolved-particle packed bed models with complex particle shapes. *Powder Technol.* **2017**, *322*, 258−272.
(32) Bender, J.; Erleben, K.; Trinkle, J. Interactive Simulation of Rigid Body Dynamics in Computer Graphics. *Comput. Graph. Forum* **2014**, *33*, 246−270.
(33) Kutscherauer, M. Particle-resolved CFD simulation of catalytic fixed bed reactors for maleic anhydride production. Ph.D. thesis, TU Clausthal, 2024.
(34) Kutscherauer, M.; Böcklein, S.; Mestl, G.; Turek, T.; Wehinger, G. D. An improved contact modification routine for a computationally efficient CFD simulation of packed beds. *Chem. Eng. J. Adv.* **2022**, *9*, No. 100197.
(35) Dhole, S.; Chhabra, R.; Eswaran, V. A numerical study on the forced convection heat transfer from an isothermal and isoflux sphere in the steady symmetric flow regime. *Int. J. Heat Mass Transfer* **2006**, *49*, 984−994.
(36) Schlichting, H.; Gersten, K. *Boundary-Layer Theory*; Springer Berlin Heidelberg: Berlin, Heidelberg, 2017.
(37) Jurtz, N.; Kraume, M.; Wehinger, G. D. Advances in fixed-bed reactor modeling using particle-resolved computational fluid dynamics (CFD). *Rev. Chem.Eng.* **2019**, *35*, 139−190.
(38) Jakobsen, H. A. *Chemical Reactor Modeling Multiphase Reactive Flows*; Springer International Publishing: Cham, 2014.
(39) Fairbanks, D. F.; Wilke, C. R. Diffusion coefficients in multicomponent gas mixtures. *Ind. Eng. Chem.* **1950**, *42*, 471−475.
(40) Fuller, E. N.; Schettler, P. D.; Giddings, J. C. New method for prediction of binary gas-phase diffusion coefficients. *Ind. Eng. Chem.* **1966**, *58*, 1827.
(41) Kutscherauer, M.; Anderson, S. D.; Böcklein, S.; Mestl, G.; Turek, T.; Wehinger, G. D. A conjugated heat and mass transfer model to implement reaction in particle-resolved CFD simulations of catalytic fixed bed reactors. *Eng. Appl. Comput. Fluid Mech.* **2024**, *18*, No. 2292100.
(42) Bosanquet, C. H. *The optimum pressure for a diffusion separation plant*; British TA Report BR-507, 1944; vol 27.
(43) Deshmukh, S. A. R. K.; Annaland, M. v. S.; Kuipers, J. A. M. Kinetics of the partial oxidation of methanol over a Fe-Mo catalyst. *Appl. Catal. A Gen.* **2005**, *289*, 240−255.
(44) Matsumoto, M.; Nishimura, T. Mersenne twister: A 623-dimensionally equidistributed uniform pseudo-random number generator. *ACM T. Model. Comput. S.* **1998**, *8*, 3−30.
(45) Lacey, P. M. C. Developments in the theory of particle mixing. *J. Appl. Chem.* **1954**, *4*, 257−268.
(46) Ullrich, C.; Bodmer, T.; Hübner, C.; Kempa, P. B.; Tsotsas, E.; Eschner, A.; Kasparek, G.; Ochs, F.; Spitzner, M. H. *VDI-Wärmeatlas*; Springer: Berlin, Heidelberg, 2013; pp 629−708.
(47) Royston, P. Remark AS R94: A Remark on Algorithm AS 181: The W-test for Normality. *J. R. Stat. Soc. Ser. C: Appl. Stat.* **1995**, *44*, 547−551.
(48) Pernicone, N. Deactivation of Fe-Mo oxide catalyst in industrial plant and simulation tests on laboratory scale. *Catal. Today* **1991**, *11*, 85−91.
(49) Gerberich, H. R.; Seaman, G. C. *Kirk-Othmer Encyclopedia of Chemical Technology*; John Wiley & Sons, Ltd, 2004.
(50) Soares, A. P. V.; Portela, M. F.; Kiennemann, A. Methanol Selective Oxidation to Formaldehyde over Iron-Molybdate Catalysts. *Catal. Rev.* **2005**, *47*, 125−174.
(51) Andersson, A.; Holmberg, J.; Häggblad, R. Process Improvements in Methanol Oxidation to Formaldehyde: Application and Catalyst Development. *Top. Catal.* **2016**, *59*, 1589−1599.
(52) Braz, C. G.; Mendes, A.; Rocha, J.; Alvim, R.; Matos, H. A. Model of an industrial multitubular reactor for methanol to formaldehyde oxidation in the presence of catalyst deactivation. *Chem. Eng. Sci.* **2019**, *195*, 347−355.
(53) Partopour, B.; Dixon, A. G. Effect of particle shape on methanol partial oxidation in a fixed bed using CFD reactor modeling. *AIChE J.* **2020**, *66*, No. e16904.
(54) Aris, R. On shape factors for irregular particles—I: The steady state problem. Diffusion and reaction. *Chem. Eng. Sci.* **1957**, *6*, 262−268.
(55) Yang, J.; Wang, Q.; Zeng, M.; Nakayama, A. Computational study of forced convective heat transfer in structured packed beds with spherical or ellipsoidal particles. *Chem. Eng. Sci.* **2010**, *65*, 726−738.
(56) Yang, J.; Wang, J.; Bu, S.; Zeng, M.; Wang, Q.; Nakayama, A. Experimental analysis of forced convective heat transfer in novel structured packed beds of particles. *Chem. Eng. Sci.* **2012**, *71*, 126−137.
(57) Dixon, A. G.; Gurnon, A. K.; Nijemeisland, M.; Stitt, E. H. CFD testing of the pointwise use of the Zehner−Schlünder formulas for fixed-bed stagnant thermal conductivity. *Int. Commun. Heat Mass Transf.* **2013**, *42*, 1−4.
(58) Peschel, A.; Jörke, A.; Sundmacher, K.; Freund, H. Optimal reaction concept and plant wide optimization of the ethylene oxide process. *Chem. Eng. J.* **2012**, *207−208*, 656−674.
(59) Maußner, J.; Pietschak, A.; Freund, H. A new analytical approximation to the extended Brinkman equation. *Chem. Eng. Sci.* **2017**, *171*, 495−499.

https://doi.org/10.1021/acsengineeringau.5c00012
ACS Eng. Au 2025, 5, 284−297